Multi-intruder structures in ^{34}P

P. C. Bender, S. L. Tabor, Vandana Tripathi, C. R. Hoffman, L. Hamilton, A. Volya, R. M. Clark, P. Fallon, A. O. Macchiavelli, S. Paschalis, M. Petri, M. P. Carpenter, R. V. F. Janssens, T. Lauritsen, E. A. McCutchan, D. Seweryniak, S. Zhu, C. J. Chiara, X. Chen, W. Reviol, D. G. Sarantites, and Y. Toh

Multi-intruder structures in ^{34}P

P. C. Bender,[1,][*] S. L. Tabor,[1] Vandana Tripathi,[1] C. R. Hoffman,[1,][†] L. Hamilton,[1] A. Volya,[1] R. M. Clark,[2] P. Fallon,[2] A. O. Macchiavelli,[2] S. Paschalis,[2] M. Petri,[2] M. P. Carpenter,[3] R. V. F. Janssens,[3] T. Lauritsen,[3] E. A. McCutchan,[3,][‡] D. Seweryniak,[3] S. Zhu,[3] C. J. Chiara,[3,4] X. Chen,[5] W. Reviol,[5] D. G. Sarantites,[5] and Y. Toh[3,6]

[1]*Department of Physics, Florida State University, Tallahassee, Florida 32306, USA*

[2]*Nuclear Science Division, Lawrence Berkeley*

National Laboratory, Berkeley, California 94720, USA

[3]*Physics Division, Argonne National Laboratory, Argonne, Illinois 60439, USA*

[4]*Department of Chemistry and Biochemistry,*

University of Maryland, College Park, Maryland 20742, USA

[5]*Chemistry Department, Washington University, St. Louis, Missouri 63130, USA*

[6]*Japan Atomic Energy Agency, Tokai, Ibaraki 319-1195, Japan*

Abstract

The available experimental information on ^{34}P has been greatly increased through the analysis of γ decays in coincidence with protons from the interaction of an ^{18}O beam at 24 MeV with an ^{18}O target. Light charged particles from the reaction were detected with Microball, and multiple γ-ray coincidences with Gammasphere. Many newly observed γ transitions have been identified and placed in the level scheme. Additionally, for most states, spins have been assigned based on measured γ-ray angular distributions while parities were inferred from lifetimes determined through Doppler-broadened line-shape analysis. Most of the states observed have been interpreted in terms of shell-model calculations using the WBP-a and SDPF-NR interactions having one particle in the $0f_{7/2}$ or $1p_{3/2}$ orbital. The two calculations agree almost equally well with the data resulting in root-mean-square differences of about 200 keV. However, a few high-lying states observed with long lifetimes challenge current calculations. Two of these may be associated with stretched $\pi f_{7/2} \otimes \nu f_{7/2}$ states, but the calculations over-predict their energies by 2 - 3 MeV. Furthermore, a newly observed long-lived 7919-keV state is established for which no explanation is available at present.

---

[*] Present address: Science Division, TRIUMF, Vancouver, British Columbia V6T 2A3, Canada; Electronic

mail: bender@triumf.ca

† Present address: Physics Division, Argonne National Laboratory, Argonne, Illinois 60439, USA

‡ Present address: National Nuclear Data Center, Brookhaven National Laboratory, Upton, New York 11973, USA

I. INTRODUCTION

The shell model using effective interactions provides the most successful interpretation of the level structure for a broad range of nuclei. However, many open questions remain; one of the most important concerns the issue of how the neutron or proton shell filling affects the shell structure of the other nucleon. This possibility was already contemplated relatively early in the history of the shell model when Talmi and Unna, while studying ^{11}Be, stated that "...the order of filling of neutron shells may depend on the proton configuration" [1]. The availability of radioactive beams has allowed considerably more exploration of such effects and what they might imply for effective interactions in nuclei farther from stability.

An excellent region to investigate how the filling of proton shells affects the neutron shell structure is in the $1s$-$0d$ shell. There are many more particle-stable nuclei available for study than in the $0p$ shell, and the universal sd-shell (USD) interaction has been shown to describe most low-lying structures well throughout this region from ^{16}O to ^{40}Ca [2]. Therefore, the experimental observation [3] that ^{31}Na is significantly more tightly bound than predicted by USD calculations suggested that one or more nucleons outside the sd shell are involved in the ground-state wave function of ^{31}Na, even though such a state is calculated to lie at a higher excitation energy in a simple shell-model picture. A subsequent determination of a revised effective interaction (USDA) [4], obtained by fitting larger data sets than were available for the USD fit, has more clearly identified a small region of nuclei with $Z \approx 10$ and $N \approx 20$ for which the ground states are more tightly bound than predicted by the pure sd calculations. This region, where intruder states expected to lie higher in the level scheme fall below the "normal" states, is often referred to as the "island of inversion".

Theoretical treatment of the island of inversion requires challenging calculations involving valence particles moving across shells and appropriate interactions including both in- and cross-shell terms. Only a few calculations have shown much success in the region. Key to refining the interactions is a more complete picture of the states that lead to inversion. A careful mapping of the intruder states in the odd-odd $Z = 15$ P isotopes can provide a valuable testing ground, as the lowest-energy, negative-parity intruder states drop steadily with increasing neutron number. The P isotopes, however, never themselves belong to the "island of inversion"; the lowest-lying, negative-parity states in ^{34}P$_{19}$ are excited to around 2.3 MeV, while the negative-parity ground-state multiplet in ^{36}P$_{21}$ should be viewed as

"normal" because the last neutron must lie above $N = 20$.

The present investigation focuses on ^{34}P, the heaviest odd-odd P isotope for which all nucleons could normally occupy the sd shell. Intruder negative-parity states with 1 particle - 1 hole (1p-1h) character were previously reported to appear at about 2.3 MeV [5–11]. Hints already existed for possible 2p-2h positive-parity states at about 6.2 MeV [9–11]. The purpose of the present work was to obtain additional experimental information on the 1p-1h states to solidify tests of shell-model descriptions and to search for other possible configurations. Overall, the present work has substantially added to the experimental information available for ^{34}P, with ten states and 24 γ transitions observed here for the first time. A clearer picture has emerged, not only due to a detailed decay scheme, but also with additional information from angular-distribution and lifetime measurements that are now available for comparison with theory. While these results have helped to strengthen the theoretical understanding of the 1p-1h intruder states, they have also generated more questions for future theoretical investigations, especially for some high-lying, long-lived states which appear to lie outside the scope of the present calculations.

Most of the previous experimental work on ^{34}P is summarized in Ref. [10]. Not listed there is an unpublished thesis using the ^{36}S(d,α) reaction [6] with polarized and unpolarized beams. Also, another investigation of ^{34}P [11] was published simultaneously with Ref. [10]. The present research using particle-γ coincidences from Gammasphere and Microball will be discussed in the context of state-of-the-art shell-model calculations in the sections that follow.

II.   EXPERIMENTAL PROCEDURE

States in ^{34}P were populated using a 24-MeV ^{18}O^{7+} beam impinging on a 260-μg/cm^2 ^{18}O target. Typical beam currents of about 30 pnA were provided by the Argonne Tandem-Linac Accelerator System (ATLAS) at Argonne National Laboratory. The ^{18}O target was produced by electrolysis of water enriched to 97% in ^{18}O on a 0.013-mm Ta backing. The Ta backing was thick enough to stop the heavy residues from the reaction, while still allowing light charged particles to pass through. Evaporated charged particles were detected using Microball [12], a nearly 4π array of 95 CsI(Tl) scintillators surrounding the target, while the γ rays emitted following the reaction were measured using Gammasphere [13], consisting

of 101 Compton-suppressed high-purity germanium detectors arranged as described in Ref [14]. The program GSSORT [14] was used to filter the data off-line into an event format suitable for use in the Florida State University analysis code GNUSCOPE [15].

The level scheme was constructed using a variety of matrices. Coincidence events between multiple γ rays detected in Gammasphere were sorted into matrices required to be in coincidence with a single proton observed in Microball and/or one or more additional γ rays corresponding to known transitions in ^{34}P. Due to the varying degree of Doppler broadening of transitions from decays occurring in the thick backing, different *styles* of matrices were created. To better observe coincidences between the longer-lived states, symmetric matrices were sorted with no Doppler correction applied. Transitions between shorter-lived levels were enhanced using symmetric matrices with both axes Doppler corrected. Additionally, for transitions between shorter-lived and longer-lived states, asymmetric matrices were sorted with a Doppler correction on only one of the two axes. The latter allows for the placement of a gate on a more easily-observed, non-shifted transition to view coincidences with Doppler corrected lines. An optimal effective recoil velocity of $v/c = 0.015$ was determined empirically for the Doppler correction.

Both Doppler-shift attenuation method (DSAM) and angular-distribution analyses of γ rays were done with data sorted into individual angles, defined by the rings of Gammasphere. The DSAM analysis was carried out with matrices sorted with a particular ring on one axis and all rings on the other. In order to reduce the effect of feeding corrections on the DSAM analysis, a combination of gating on transitions feeding the one of interest from a higher-energy level and, when possible, only gating on the in-flight components of those transitions was used. Lifetimes were deduced by comparing the lineshapes measured at 50.07° and 129.93° with those simulated by the program FITS [16] for a variety of lifetime hypotheses. Stopping powers were obtained from the SRIM software package [17]. The measured lifetimes of states above the one of interest were included in the simulations. When it was not possible to gate from above to eliminate the effects of side feeding, the effective lifetime of the later was inluded in the fits. Typically, gating from below resulted in line shapes with sufficient counts to provide a precise fit of the lifetime for the level of interest and for the side feeding. For cases in which gating above and below were possible, the level lifetimes obtained from the two fits were found to be in agreement within the quoted uncertainties. Also the lifetimes inferred from the independent determinations from the forward and backward angles were

always found to agree well within the quoted errors, and the average of the two values is reported in Table I.

Angular distributions were measured for most of the γ transitions. The angular-distribution analysis was performed with data from the forward and backward symmetric angles combined, taking advantage of the natural alignment provided by fusion reactions. The distribution of magnetic sub-states populated in each state was estimated as a Gaussian distribution with a width $\sigma = 1.41$ in a method similar to that in Ref. [18]. The measured angular distributions were compared with calculations using the code AD [16] for different hypotheses of initial spin. The code calculates the expected angular distributions using the formulation of Ref. [18]. The effects of attenuation of the angular distribution due to finite detector sizes are included. The goodness of fit χ^2 was calculated for all mixing ratio values δ from minus to plus infinity. The information this comparison provides about the spins of the parent states is discussed in the following sections.

III. EXPERIMENTAL RESULTS

The results for ^{34}P from the present experiment are summarized in Fig. 1 and in Table I. States and transitions not previously reported are shown in red (online) in all figures. The high statistics in the present experiment allowed us to confirm most of the previous results.

The states below 2 MeV have been relatively well understood in the past and the present results are consistent with previous work discussed in detail in Ref. [10]. Many states above this excitation energy require further discussion, starting with the level at 2229 keV. A state at 2225(10) keV was first reported in the ^{34}S(t,^{3}He) study in Ref. [5]. A state of similar energy, 2231(10) keV, was observed in a ^{36}S(d,α) reaction study [6]. Later, in an intermediate-energy Coulomb excitation experiment [8], γ transitions of 422(7) and 627(9) keV were observed with a NaI array. The 422(7)-keV line was identified as the 429-keV transition seen in Ref. [5], while the 627(9)-keV line was suggested as a transition from the 2235-keV level to the 1608-keV state, even though the intervening 1179-keV decay between the levels at 1608 and 429 keV was not seen. This was believed to be due to a lower detector efficiency and to the limited statistics and resolution reported for the NaI detectors [8].

In the present work, a 2229-keV state is firmly established through decays to each of the three lower levels. All three γ transitions are seen in the spectrum gated by the 1524-keV

TABLE I. Summary of experimental data on ^{34}P. The column E_x denotes an observed energy level with a deduced spin-parity of J_i^π that decays via a transition E_γ to a level with spin-parity of J_f^π. Also listed in the Table is the mean lifetime, τ, of the state E_x. The best value of the arctan of the mixing ratio, δ, for a transition between J_i^π and J_f^π is also given. The a_2 and a_4 coefficients are from an unconstrained Legendre polynomial fit to the data. These values are given as a representation of the data and are independent of the angular-distribution analysis which led to the determination of δ.

| E_x	E_γ	J_i^π	J_f^π	Mean τ	a_2	a_4	arctan(δ)
(keV)	(keV)			(ps)			(deg)
429.1(2)	429.1(2)	2^+	1^+	1.9^{+9}_{-5}	-0.09(3)	0.02(4)	-6(7)
1608.2(5)	1179.1(4)	1^+	2^+	0.75^{+65}_{-20}	-0.03(3)	0.01(4)	
	1608(1)		1^+				
2228.8(6)	620.6(4)	$2^{(-)}$	1^+	> 3	-0.12(8)	0.06(10)	-4(9)
	1799.7(6)		2^+				
	2229(1)		1^+				
2305.0(5)	1875.9(4)	4^-	2^+	2900(150)[a]	0.32(6)	0.02(8)	0(7)
2320.5(6)	1891.4(5)	3^-	2^+	> 10	-0.15(7)	0.03(8)	-4(8)
3352.4(7)	1031.7(7)	5^-	3^-				
	1047.5(4)		4^-	0.52^{+18}_{-12}	-0.23(7)	0.04(8)	-1(5)
3752.4(9)	1431.8(6)	$(3,4)^-$	3^-	0.37(8)			
	(1446)		4^-				
	1523.9(9)		$2^{(-)}$				
3911(1)	1591(1)	$(3,4)^-$	3^-	0.2(1)			
3951.4(7)	1631.5(11)	5^-	3^-				
	1646.1(4)	5^-	4^-	0.16(5)	-0.31(7)	0.01(8)	2(10)
4447(2)	2126(2)	$(4)^-$	3^-	< 0.14			
4630(1)	678.7(4)	6^-	5^-	0.44(7)	-0.05(8)	0.03(8)	-7(6)
	2325.1(6)		4^-		0.42(8)	-0.05(8)	-1(6)
5013(2)	2692(2)	$(2)^-$	3^-	< 0.1			
5281(2)	2960(2)	$(3)^-$	3^-	< 0.1			

[a] Ref. [21]

7
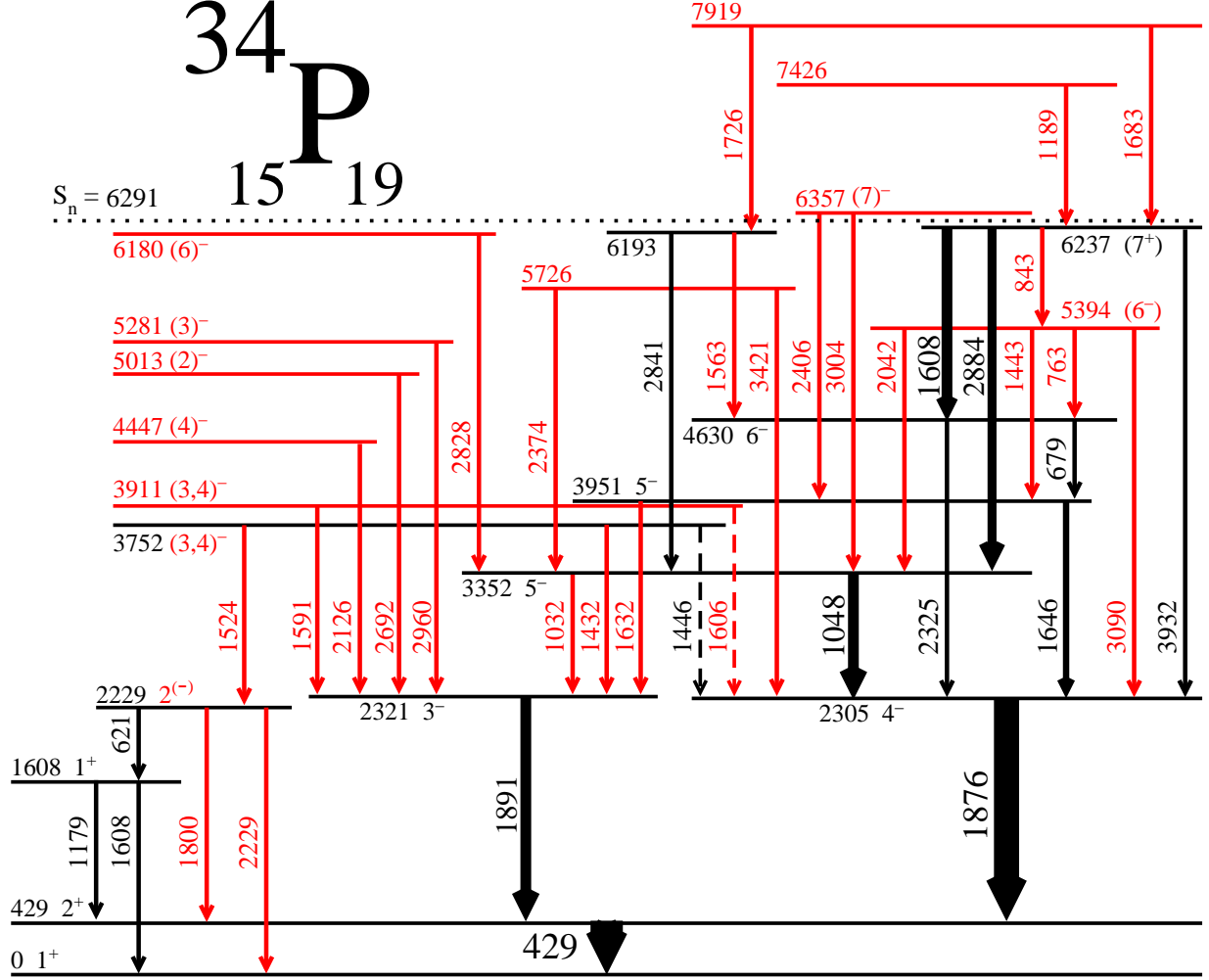
FIG. 1. (Color online) The level scheme of ^{34}P based on the present data. States and transitions in red are new to this work; arrow widths are proportional to the observed γ-ray intensities. All J^π values listed in the Figure are derived from observed results; if no results could be reliably extracted from the data, no J^π value is given.

γ line that feeds into the 2229-keV level [see Fig. 2 (a)]. This demonstrates that all three decays come from a single state and not from a closely spaced doublet. The goodness-of-fit curves from the angular distribution of the 621-keV γ line from the 2229-keV state [see Fig. 3(a)] favor a $2\hbar \to 1\hbar$ transition and rule out a spin of $3\hbar$ for the 2229-keV state. The line shape of the 621-keV decay does not indicate an in-flight component. However, because of the fact that the 621-keV transition rides on a $n - n'$ γ line shape, only a conservative lifetime limit of $\tau > 3$ ps [see Table I] could be determined. These weak decay strengths to

TABLE I. *Continued.*

E_x	E_γ	J_i^π	J_f^π	Mean τ	a_2	a_4	$\arctan(\delta)$
(keV)	(keV)			(ps)			(deg)
5394(1)	762.9(8)	(6^-)	6^-				
	1442.6(7)		5^-	0.16^{+12}_{-7}	-0.24(9)	0.12(10)	-1(3)
	2042(1)		5^-		-0.21(12)	0.26(15)	-3(8)
	3090(2)		4^-				
5726(2)	2373.9(15)		5^-				
	3421(2)		4^-				
6180(2)	2828(2)	$(6)^-$	5^-	< 0.1			
6193(2)	1563.4(14)		6^-				
	2841(2)		5^-				
6237(1)	842.5(6)	(7^+)	(6^-)	> 10	-0.19(12)	-0.02(12)	-3(8)
	1607.9(5)		6^-		-0.17(10)	0.11(11)	-3(5)
	2884.3(7)		5^-		0.52(10)	-0.05(11)	-6(10)
	3932(3)		4^-				
6357(1)	2405.9(7)	$(7)^-$	5^-	< .05	-0.53(12)	-0.57(13)	
	3004(2)		5^-				
7426(2)	1189(2)		(7^+)	< 0.1			
7919(2)	1683(1)		(7^+)	> 0.5			
	1726(1)						

positive-parity states [see Table II] strongly suggest negative parity for the 2229-keV level. A negative-parity assignment for this state rules out $1\hbar$ as the initial spin because the large mixing ratio would imply an improbably large $M2$ strength. In contrast, the lifetime of the 3752-keV state observed to feed this state by the 1524-keV transition is measured through a separate decay branch (1432 keV) to the confidently assigned 3^- state at 2321 keV as 0.37 ps [see Figs. 4(a,b)]. Observing this relatively short mean lifetime not only implies a negative parity for the 3752-keV state, but also asserts that there is no parity change in the 1524-keV decay to the 2229-keV level. Together the present experimental evidence provides an assignment of $2^{(-)}$ for the 2229-keV level. This is consistent with the assignment
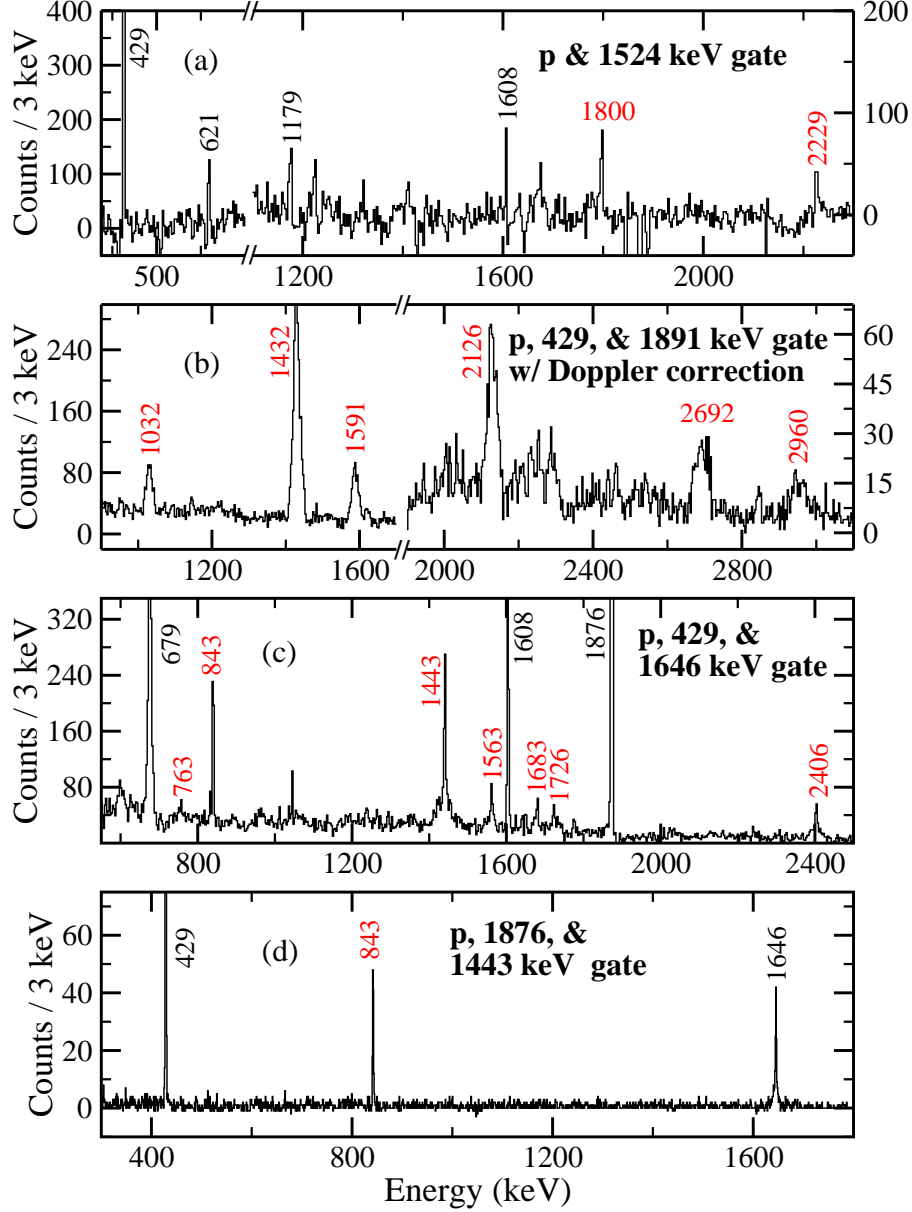
FIG. 2. (Color online) Portions of the γ spectra in coincidence with the indicated gates, where p stands for a proton gate. Conclusions based on these spectra are discussed in the text.

of unnatural parity in Ref. [6], but may not be consistent with the observed population in the Coulomb excitation experiment of Ref. [8]. Conceivably, a different state was populated in Ref. [8], although the possibility of negative parity was mentioned in Ref. [19].

The assignment of 3^- to the 2321-keV state was already rather firm before the present work. The decay line at 1891 keV in the present data exhibits no sign of a Doppler shift, implying a mean lifetime longer than 10 ps. The angular distribution is fitted well with a
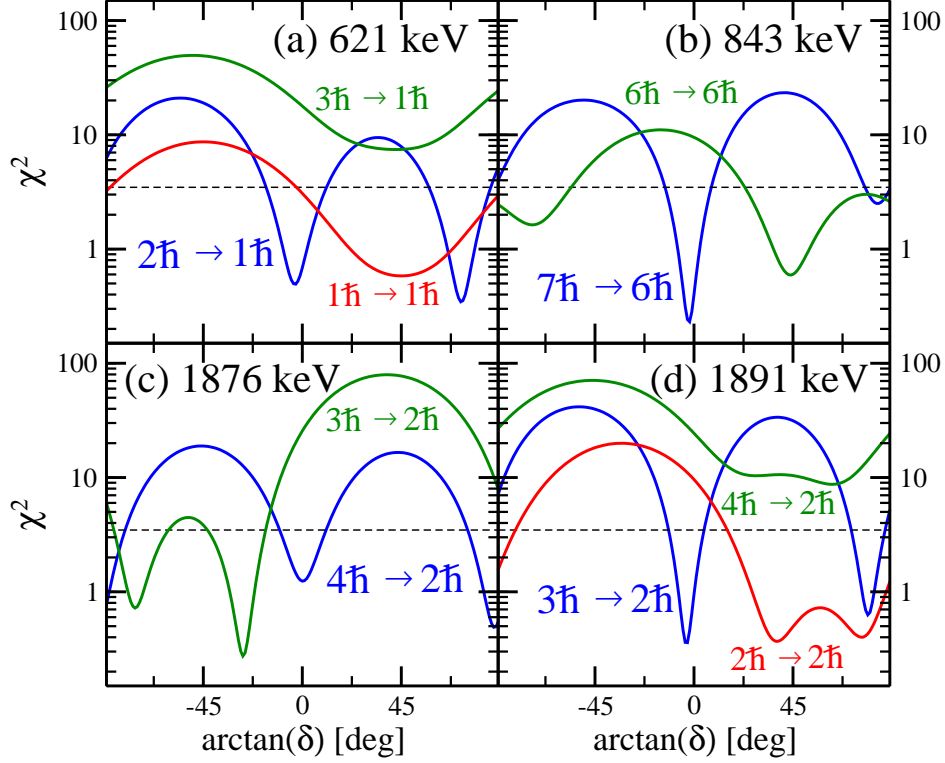
FIG. 3. (Color online) Fits to some representative angular distributions. The reduced goodness-of-fit χ^2 is graphed as a function of the mixing ratio δ between the spin combinations shown. The horizontal dashed line on each graph is the 0.1% confidence level.

$3\hbar \to 2\hbar$ hypothesis with essentially zero mixing ratio [see Fig. 3(d)]. A $4\hbar \to 2\hbar$ transition is ruled out and a $2\hbar \to 2\hbar$ possibility is less likely because of the large δ value it would imply. Likewise, the 4^- assignment to the 2305-keV state, which decays by the 1876-keV transition, is also firm, though not without some controversy in past work. First confidently proposed as 4^- in Ref. [9], this assignment was changed in the work of Ref. [20] to 4^+. The 2305-keV level was subsequently reverted to 4^- in Ref. [10] and $4^{(-)}$ in Ref. [11]. Figure 3(c) in the present work indicates that the 1876-keV transition is fitted well with a zero mixing ratio similar to Ref. [10], although the other minimum in χ^2 at $\arctan(\delta) = 90°$ for infinite mixing ratio (pure $E3$ decay) gives a somewhat better fit. A recent direct measurement of the half life of the 2305-keV level gave a value of 2.0(1) ns [$i.e.$ a mean life of 2.90(15) ns] [21]. This yields a reasonable $M2$ decay strength of 0.064(6) Weisskopf units (W.u.) ($\delta = 0$). The χ^2 minimum at $\arctan(\delta) = 90°$ for pure $E3$ decay would imply a physically unreasonable $B(E3)$ value of over 100 W.u. Thus the current evidence supports the 4^-
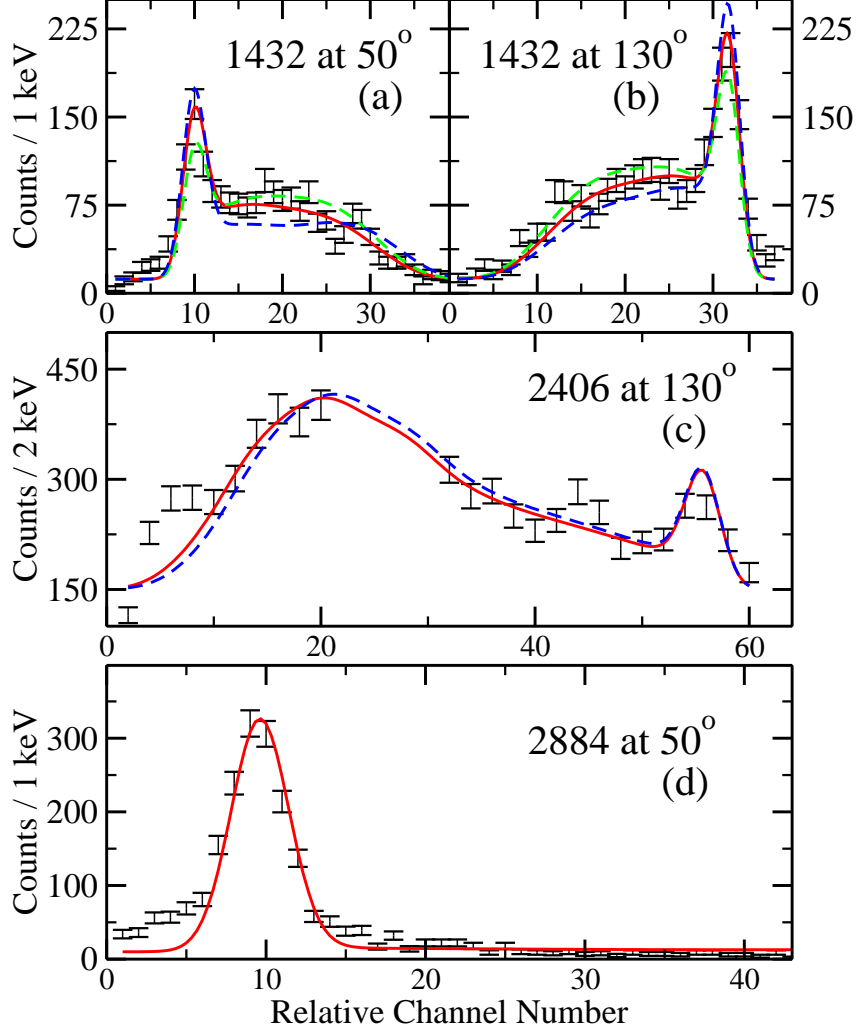
FIG. 4. (Color online) Representative Doppler-shifted decay line shapes and simulations. The dispersion of the x-axis is 1 keV/channel in panels (a), (b), and (d) and 2 keV/channel for (c). The red curves (solid lines) represent the best fits and correspond to the mean lifetimes listed in Table I. The other curves (dashed lines) show one standard deviation uncertainties. [For (c) the missing data points are due to the presence of a known contaminant.]

assignment for the 2305-keV state with an essentially pure $M2$ decay to the first excited state.

A number of new γ transitions were observed decaying into the 2321-keV, 3^- level by placing a double coincidence gate on the 429- and 1891-keV transitions and applying an approximate correction for the Doppler shifts, as presented in Fig. 2(b). Although many of the peaks are still broad, their widths have been reduced considerably by the Doppler

correction. The lineshapes of these transitions yield short lifetimes or limits as indicated in Table I. The $B(E1)$ values associated with these lifetimes were calculated to be greater than 2 - 4 $E-4$ Weisskopf units (W.u.), much larger than expected in this mass region. Thus no parity change is assumed in their decays to the 3^- level and hence negative parities for the parent states.

The 1432-keV line establishes a state at 3752 keV whose 1524-keV decay to the 2229-keV level was discussed above. The 3752-keV state is shown in black in Fig. 1, since a state at 3749 keV was proposed in Ref. [11], based on a 1444-keV decay to the 2305-keV level. However, the 1443-keV line in the present data is clearly in coincidence with the 1646-keV decay [see Figs. 2(c) and (d)]. These coincidence relationships and three other decay branches establish a new level at 5394-keV. While the bulk of the γ intensity around 1443 keV comes from the 5394-keV $\rightarrow$ 3951-keV decay, the present data can neither rule out, nor support, a weak 3752-keV $\rightarrow$ 2305-keV branch at 1446 keV. The latter decay is proposed as a dashed line in the level scheme in view of its uncertainty.

Some examples of line-shape fits used to determine mean lifetimes of the levels can be found in Fig. 4. The values obtained are listed in Table I. Mean lifetimes of most of the states above 2500 keV are typically shorter than 1 ps. Therefore, the few higher-energy states with much longer lifetimes stand out as potentially having unique structure or spin. One of these "special" states lies at 6237 keV. The present work confirms a third decay branch at 3932 keV reported in Ref. [11] and adds a fourth branch at 843 keV [Fig. 2(d)]. The γ transitions display no sign of a Doppler shift, as can be seen in Fig. 2(d), and Fig. 4(d). Angular distributions for the 843- and 2884-keV γ transitions strongly suggest a spin of $7\hbar$. A spin of $6\hbar$ is not completely ruled out, but would imply a large mixing ratio which is unlikely for the 843-keV decay [Fig. 3(b)].

Three states were observed above the ^{34}P neutron separation energy of 6291(5) keV [22]. Only a significant angular-momentum barrier can suppress their neutron decay sufficiently to result in observable electromagnetic decay branches. Particularly interesting is the highest-energy state observed at 7919 keV. Its two decay branches can be seen in Fig. 5. Both are narrow lines with no indication of Doppler broadening within the limited statistics of this high lying state, again implying de-excitation from a rather long-lived state.
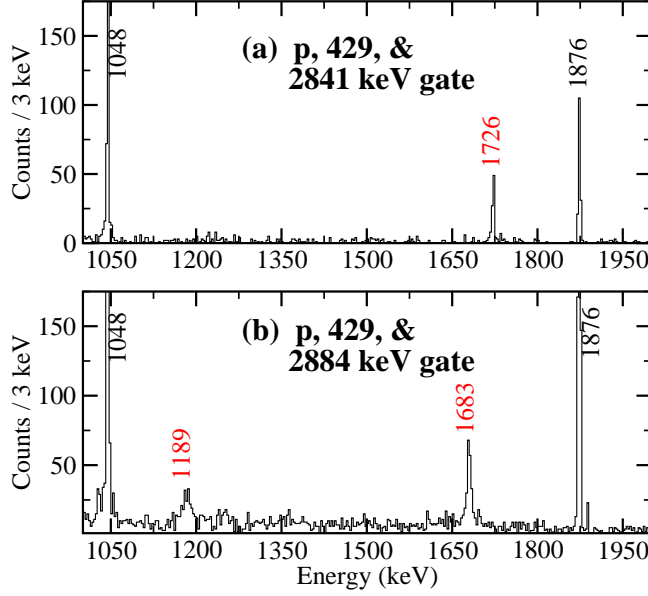
FIG. 5. (Color online) Portions of the γ spectra in coincidence with one proton (p), a 429-keV γ line, and a second γ line as indicated.

IV. DISCUSSION AND SHELL-MODEL ANALYSIS

A comparison of the lowest few positive- and negative-parity states in the even P isotopes is presented in Fig. 6. The most obvious trend is the steady decrease in energy of the negative-parity states with increasing neutron number N until they reach the ground state at $N = 21$, where at least the last unpaired neutron must lie in the fp shell. It is also interesting to note that the lowest 2^-, 3^-, and 4^- states remain closely clustered together even though, theoretically, not all the same orbitals are involved.

Focusing on ^{34}P, the lowest three positive-parity levels are well reproduced [10] by shell-model calculations limited to the $0d$-$1s$ shell using the USD interaction [2]. In the present discussion, such states will be called 0-particle-0-hole or 0p-0h states. Many such 0p-0h states are calculated, but there is no evidence that any more have been seen in the current work. Rather, the next three excited states are of negative parity, and calculations discussed below indicate that they can be associated with configurations involving the promotion of one particle to the higher $0f_{7/2}$ or $1p_{3/2}$ orbitals (1p-1h states). Most of the states seen above 2 MeV appear to be of this type. The possibility that a few of the highest states with abnormally long lifetimes are based on 2p-2h or even 3p-3h configurations will be discussed
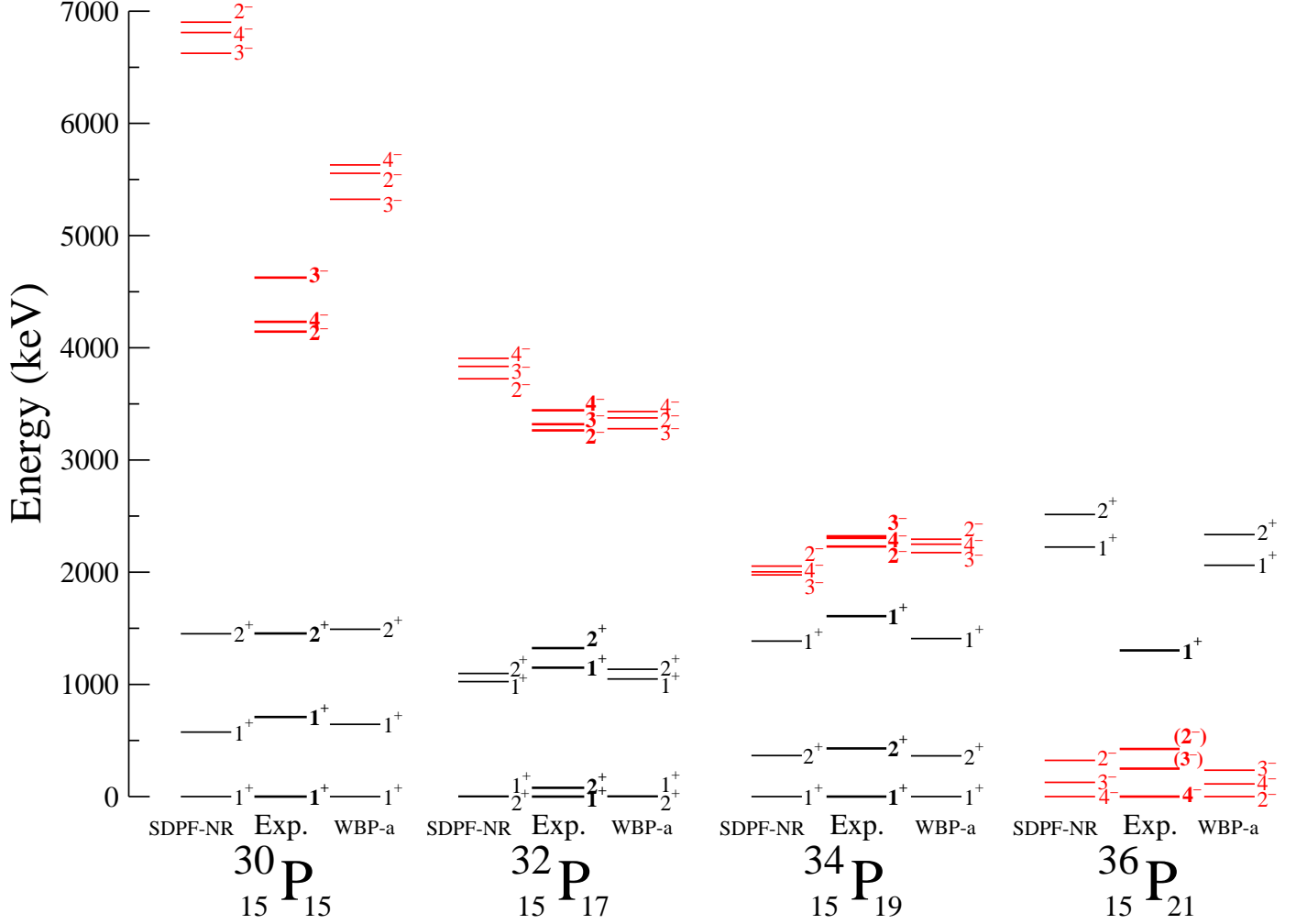
14

FIG. 6. (Color online) A comparison of data for the lowest positive- and negative-parity states across the even P isotopes with the two shell-model calculations discussed in the text. The observed and calculated (based theoretically on 0p-0h or pure sd configurations) positive-parity states are given in black. The observed and calculated (based on 1p-1h configurations) negative-parity levels are in red(online). Experimental information on excited states of ^{30}P, ^{32}P, and ^{36}P is taken from Refs. [23–26]. A more complete listing of calculated states in ^{34}P is given in Table III of Ref. [10].

below.

The relatively low energies of the intruder 1p-1h states in ^{34}P provide part of the explanation for the dearth of 0p-0h states observed in the experiment. Another contribution is the well-established tendency of heavy-ion reactions to favor population of higher-spin states combined with the ability of any occupation of the $f_{7/2}$ orbital to generate higher spin in

this mass region.

A modified WBP shell-model interaction called WBP-a was introduced in Ref. [10]. The modification consisted of reducing the $0f_{7/2}$ and $1p_{3/2}$ single-particle energies (which were not well determined in the original WBP fit to nuclei in the mass 20 region) by 1.8 and 0.5 MeV, respectively, to better reproduce the ^{32}P level scheme. The WBP-a interaction was found to also work well for the 1p-1h negative-parity states in ^{34}P. A similar need for the reduction of the $0f$-$1p$ single particle energies by 0.7-1.0 MeV in the WBP interaction has also been reported in a recent study by Brown *et al.*, trying to explain the level schemes of ^{25,27}Ne and ^{29}Mg [27]. As discussed in Ref. [10], the close spacing and nearly identical calculated structures of the lowest 3^- - 4^- doublet in ^{34}P conform well to the expected $\pi s_{1/2} \otimes \nu f_{7/2}$ configuration. Although the $\pi s_{1/2} \otimes \nu p_{3/2}$ configuration might be expected to give a closely spaced doublet of 1^- and 2^- states above this, the 1^- state is instead predicted to be about 0.5 MeV higher than the 2^-. The larger energy splitting apparently results from about 30% mixing of the $\pi s_{1/2} \otimes \nu f_{7/2}$ configuration in the 2^- state, lowering its energy, compared to $\approx$13% for the 1^- state, as indicated in Table III of Ref. [10].

It should be noted that the WBP-a calculations predict a 2^+, 0p-0h state at 2216 keV and a 2^-, 1p-1h state nearby at 2294 keV. Both of these energies are well within the typical theoretical uncertainty of 150 keV with respect to the 2229-keV experimental level. The possibility that the 2229-keV state could be associated with the predicted 2_2^+ level was considered carefully and a search for evidence of a second $2\hbar$ state around 2229 keV was undertaken. No such level was found, and, as shown above, the experimental evidence strongly favors negative-parity for the 2229-keV state.

We have also performed calculations with the more commonly used SDPF-NR interaction [28], because the WBP-a interaction was adjusted by changing single-particle energies to fit states in ^{32}P and has not yet been compared to a wide range of nuclei. On the other hand, the SDPF-NR interaction accounts for the shell evolution as a function of neutron excess by changing its monopole interactions. The two calculations thus provide an opportunity to compare different approaches for treating cross-shell interactions, namely adjusting the single-particle energies versus modifying the monopole mean field. The WBP-a and SDPF-NR calculations are compared with experiment for the lowest positive- and negative-parity states in Fig. 6. The predictions of the two interactions for the 0p-0h positive-parity states are similar as both were constructed with the aim of reproducing the predictions of the USD

interaction. The two calculations reproduce the general trend of the close clustering of the $2^-, 3^-, 4^-$ triplet and its decrease in excitation energy with increasing N. However, both over-predict the magnitude of the decrease, although somewhat less so for WBP-a. The WBP-a results are the closest for ^{32,34}P, but one should remember that the single-particle energies were adjusted specifically to optimize this agreement.

The states and decays observed in ^{34}P are compared with the corresponding theoretical results, calculated using both the WBP-a and SDPF-NR interactions, in Table II. These calculations involved 0, 1, or 2 particles (protons or neutrons) in the $0f_{7/2}$ and $1p_{3/2}$ orbitals, giving 0p-0h, 1p-1h, and 2p-2h states, respectively. A correspondence is evident for the states with experimentally assigned spins and parities. In many other cases, similarities between the predicted and observed energies and decay branching ratios provide strong model-dependent identifications and spin-parity assignments. These additional assignments are listed in Table II, but are not given in Fig. 1. Where the model-dependent identifications are not as conclusive, the spin assignments have been placed in parentheses in Table II. For a few levels, it was not possible to select a matching theoretical state with any confidence and no J_i value is suggested as a result.

In the first three columns of Table II, the measured and predicted excitation energies are compared. The comparison for the branching ratios can be found in the middle columns. Branches are only shown for the experimentally observed decay paths and the theoretical branching ratios do not always add up to 100% as a result. In two cases, only a question mark is indicated in the Table for the experimental branching ratio, due to the presence of a doublet where, despite the use of different coincidence gates, the (probably weak) intensity of that member of the doublet could not be extracted reliably. The electromagnetic transition strengths in Weisskopf units (W.u.) are provided in the last three columns. The theoretical $B(\lambda)$ values are based on standard magnetic moments and effective charges of 1.5 and 0.5 e for protons and neutrons, respectively.

The root-mean-square (RMS) differences between the experimental energies and the shell-model predictions with the WBP-a and SDPF-NR interactions are 193 and 214 keV, respectively. These values are very similar to each other and comparable to the RMS differences seen for positive-parity, 0p-0h pure sd states in ^{30}Al, for instance, where the RMS differences of 265, 175, and 173 keV were reported for comparisons of data with the USD, USDA, and USDB interactions, respectively [29]. Hence, one can conclude that the WBP-a and SDPF-

NR interactions are almost equally successful in describing the negative-parity, 1p-1h states in ^{34}P.

With satisfactory shell-model descriptions of the 0p-0h and 1p-1h states in ^{34}P, it is clear that the challenge resides with the 2p-2h states. The 6237-keV state was first reported in Ref. [9], where a 7^+ stretched $\pi f_{7/2} \otimes \nu f_{7/2}$ configuration was proposed. The present work agrees with this spin-parity assignment, which also accounts for its relatively long lifetime. Another tentative 7^+ state has been identified in the present work at 6193 keV. The WBP-a shell-model calculations predict two 7^+ states arising from 2p-2h excitations at 7994 and 8470 keV. These are the only lower-lying 2p-2h states with appreciable $f_{7/2}$ proton occupancy (0.27 and 0.13 for the two cases). These calculated 2p-2h levels lie well below the predicted 0p-0h, 7^+ state at 11.4 MeV, but are about 2 MeV above the experimental levels. Calculations in a model space allowing mixing between the 0p-0h and 2p-2h states do not alter the results significantly. Since the two-body matrix elements in the WBP-a interaction were not adjusted to reproduce 2p-2h states in this region, it would be interesting to explore in future theoretical work how their optimization might improve agreement with such states. Calculations using the SDPF-NR interaction are rather similar, except that the lowest 7^+ state is predicted at 8802 keV with a $\pi f_{7/2}$ proton occupancy of 0.23.

The other long-lived state which awaits a satisfactory interpretation is the highest level seen at 7919 keV. Interestingly, it decays only to the two proposed 7^+ states. This state does not have a straightforward counterpart in any of the calculations. One may speculate that this state involves three particles above the $N = 20$ gap (3p-3h). However, it would then be difficult to understand why such a negative-parity state would decay only to 7^+ states when a 7^- state is predicted at about the same energy. The $g_{9/2}$ orbital carries high angular momentum and a fully aligned $\pi g_{9/2} \otimes \nu g_{9/2}$ configuration could result in a spin-parity of 9^+, but would be expected to be associated with relatively fast $E2$ decays to the two 7^+ states. Clearly a satisfactory explanation will have to await further work.

V. SUMMARY

The present work has substantially increased the experimental information available on ^{34}P, a nucleus close to the island of inversion. High-spin states were populated in the ^{18}O + ^{18}O reaction. The charged-particle detector array Microball provided channel selection

TABLE II. A comparison of experimental and theoretical energies and electromagnetic transition strengths. The letter "E" is used to denote experimental quantities, and "W" and "S" point to shell model predictions using the WBP-a and SDPF-NR interactions, respectively. The $B(\lambda)$ transition probabilities are for the indicated multipolarity λ, which is the lowest allowed based on the spin assignments. Spin-parity assignments in this table are based on shell-model considerations as well as experimental data. Spin values in parentheses indicate that the comparisons of experimental and theoretical energies and branching ratios are not as definitive as for the other states.

E_x(E) (keV)	E_x(W) (keV)	E_x(S) (keV)	E_γ(E) (keV)	J_i^π	J_f^π	BR(E)	BR(W)	BR(S)	λ	$B(\lambda)$E (W.u.)	$B(\lambda)$W (W.u.)	$B(\lambda)$S (W.u.)
429	363	366	429	2_1^+	1_1^+	100	100	100	$M1$	0.21_{-7}^{+8}	0.33	0.32
1608	1408	1386	1179	1_2^+	2_1^+	66(3)	66		$M1$	0.017_{-7}^{+6}	0.005	0.005
			1608		1_1^+	34(3)	34		$M1$	0.004_{-2}^{+1}	0.001	0.001
2229	2294	2054	621	2_1^-	1_2^+	30(6)			$E1$	$< 4\cdot10^{-4}$		
			1800		2_1^+	44(7)			$E1$	$< 2.5\cdot10^{-5}$		
			2229		1_1^+	26(6)			$E1$	$< 8\cdot10^{-6}$		
2305	2249	2003	1876	4_1^-	2_1^+	100			$M2$	0.064(6)	0.15	0.12
2321	2175	1976	1891	3_1^-	2_1^+	100			$E1$	$< 1.5\cdot10^{-4}$		
3352	3576	3206	1032	5_1^-	3_1^-	2(1)	12	4	$E2$	4(1)	2.6	2.2
			1048		4_1^-	98(1)	88	96	$M1$	0.052_{-13}^{+16}	0.02	0.02
3752	4070	3871	1432	$(3_3)^-$	3_1^-	93(2)	23	71	$M1$	0.027(6)	0.03	0.04
			(1446)		4_1^-	?	59	4	$M1$		0.078	0.022
			1524		2_1^-	7(2)	14	24	$M1$	0.0015(4)	0.014	0.016
3911	3877	3685	1591	$(4_3)^-$	3_1^-	100	37	54	$M1$	0.040_{-16}^{+26}	0.014	0.005
			(1606)		4_1^-	?	63	33	$M1$		0.003	0.044
3951	4084	3802	1632	5_2^-	3_1^-	4(2)	4	1	$E2$	3.4_{-10}^{+13}	1.8	1.9
			1646		4_1^-	96(2)	95	98	$M1$	0.04(2)	0.08	0.12
4447	4865	4692	2126	$(4_4)^-$	3_1^-	100	75	74	$M1$	> 0.024	0.06	0.07
4630	4792	4562	679	6_1^-	5_2^-	35(3)	27	35	$M1$	0.085(15)	0.18	0.11
			2325		4_1^-	65(3)	68	46	$E2$	2.6(5)	2.8	2.4

TABLE II. *Continued.*

E_x(E) (keV)	E_x(W) (keV)	E_x(S) (keV)	E_γ(E) (keV)	J_i^π	J_f^π	BR(E)	BR(W)	BR(S)	λ	$B(\lambda)$E (W.u.)	$B(\lambda)$W (W.u.)	$B(\lambda)$S (W.u.)
5013	4932	4916	2692	2_5^-	3_1^-	100	86	75	$M1$	> 0.016	0.088	0.085
5281	5462	5569	2960	$(3_7)^-$	3_1^-	100	47	47	$M1$	> 0.014	0.026	0.029
5394	5710	5299	763	6_2^-	6_1^-	8(3)	8	5	$M1$	0.027^{+20}_{-12}	0.097	0.086
			1443		5_2^-	54(6)	43	53	$M1$	0.036^{+27}_{-16}	0.069	0.11
			2042		5_1^-	24(5)	29	30	$M1$	0.006^{+5}_{-3}	0.003	0.018
			3090		4_1^-	15(5)	15	11	$E2$	0.4^{+3}_{-2}	0.40	0.78
5726			2374		5_1^-	78(6)						
			3421		4_1^-	22(6)						
6180	6115	5946	2828	6_3^-	5_1^-	100	82	87	$M1$	> 0.014	0.094	0.075
6193	7994	8802	1563	(7_1^+)	6_1^-	33(7)						
			2841		5_1^-	67(7)						
6237	8470	9109	843	(7_2^+)	6_2^-	19(4)			$(E1)$	$< 2 \cdot 10^{-5}$		
			1608		6_1^-	40(5)			$(E1)$	$< 1 \cdot 10^{-5}$		
			2884		5_1^-	36(5)			$(M2)$	< 0.8		
			3932		4_1^-	5(3)			$(E3)$	< 6		
6357	6628	6305	2406	7_1^-	5_2^-	43(8)			$E2$	> 18	1.4	1.2
			3004		5_1^-	57(8)			$E2$	> 4	4.6	3.0
7426			1189		(7_1^+)	100						
7919			1683		(7_1^+)	67(4)						
			1726		(7_2^+)	33(4)						

and electromagnetic radiation was detected with Gammasphere. In addition to greatly expanding the level scheme, the experiment provided valuable angular distributions and lifetime information for many of the transitions and levels. As a result, firm spin and parity assignments were possible for many excited states.

The experimental results have been compared with shell-model calculations using two interactions appropriate to this mass region, WBP-a and SDPF-NR. The ground state and the first two excited states are the only pure sd or 0p-0h states observed. Above these,

starting around 2 MeV, essentially all the observed levels have negative parity and, thus, involve neutrons occupying "intruder" orbitals above the sd shell. These states are described relatively well by shell-model calculations using both the WBP-a and SDPF-NR interactions with RMS differences around 200 keV. The WBP-a interaction does a slightly better job of reproducing the variation with neutron number of the energies of the lowest $2^-, 3^-, 4^-$ triplet, although both interactions overestimate this trend to varying degrees. In contrast to the good description of 0p-0h and 1p-1h states, both interactions exhibit substantial limitations in their predictive power of higher-energy, higher-spin levels where 2p-2h states can occur. It was shown that the long-lived 6237- and 6193-keV levels are most likely $J^\pi = 7^+$ states with a substantial contribution of the stretched $\pi f_{7/2} \otimes \nu f_{7/2}$ configuration. The WBP-a interaction over-predicts the energies of such states by almost 2 MeV with a $\pi f_{7/2}$ occupancy of only 0.27. Adjustment of the two-body matrix elements of the interaction might improve agreement, but theoretical efforts in that direction have not yet been carried out. The long-lived 7919-keV state presents an even bigger challenge for future theoretical work.

ACKNOWLEDGMENTS

[1] I. Talmi and I. Unna, Phys. Rev. Lett. **4**, 469 (1960).

[2] B. H. Wildenthal, M. S. Curtin, and B. A. Brown, Phys. Rev. C 28, 1343 (1983).

[3] C. Thibault, R. Klapisch, C. Rigaud, A. M. Poskanzer, R. Prieels, L. Lessard, and W. Reisdorf, Phys. Rev. C **12**, 644 (1975).

[4] B. A. Brown and W. A. Richter, Phys. Rev. C **74**, 034315 (2006).

[5] F. Ajzenberg-Selove, E. R. Flynn, and J. W. Sunier, Phys. Rev C **15**, 1 (1977).

[6] A. J. Trudel, Ph.D. dissertation, McMaster University, 1987.

[7] B. Fornal, R. H. Mayer, I. G. Bearden, Ph. Benet, R. Broda, P. J. Daly, Z. W. Grabowski, I Ahmad, M. P. Carpenter, P. B. Fernandez, R. V. F. Janssens, T. L. Khoo, T. Lauritsen, E. F. Moore, and M. Drigert, Phys. Rev. C **49**, 2413 (1994).

[8] B. V. Pritychenko, T. Glasmacher, B. A. Brown, P. D. Cottle, R. W. Ibbotson, K. W. Kemper, and H. Scheit, Phys. Rev. C **62**, 051601(R) (2000).

[9] J. Ollier, R. Chapman, X. Liang, M. Labiche, K.-M. Spohr, M. Davison, G. de Angelis, M. Axiotis, T. Kröll, D. R. Napoli, T. Martinez, D. Bazzacco, E. Farnea, S. Lunardi, A. G. Smith, and F. Haas, Phys. Rev. C **71**, 034316 (2005).

[10] P. C. Bender, C. R. Hoffman, M. Wiedeking, J. M. Allmond, L. A. Bernstein, J. T. Burke, D. L. Bleuel, R. M. Clark, P. Fallon, B. L. Goldblum, T. A. Hinners, H. B. Jeppeson, Sangjin Lee, I-Y Lee, S. R. Lesher, A. O. Macchiavelli, M. A. McMahan, D. Morris, M. Perry, L. Phair, N. D. Scielzo, S. L. Tabor, Vandana Tripathi, and A. Volya, Phys. Rev. C **80**, 014302 (2009).

[11] R. Chakrabarti, S. Mukhopadhyay, Krishichayan, A. Chakraborty, A. Ghosh, S. Ray, S. S. Ghugre, A. K. Sinha, L. Chaturvedi, A. Y. Deo, I. Mazumdar, P. K. Joshi, R. Palit, Z. Naik, S. Kumar, N. Madhavan, R. P. Singh, S. Muralithar, B. K. Yogi, and U. Garg, Phys. Rev. C **80**, 034326 (2009).

[12] D. G. Sarantites, P.-F. Hua, M. Devlin, L. G. Sobotka, J. Elson, J. T. Hood, D. R. LaFosse, J. E. Sarantites, and M. R. Maier, Nucl. Instrum. Methods Phys. Res. A **381**, 418 (1996).

[13] I-Y. Lee, Nucl. Phys. **A520**, 641c (1990).

[14] http://www.phy.anl.gov/gammasphere.

[15] J. Pavan, Ph.D. dissertation, Florida State University, 2004.

[16] E. F. Moore, Ph.D. dissertation, Florida State University, 1988.

[17] http://www.srim.org (2008); J. F. Ziegler, J. P. Biersack, and U. Littmark, *The Stopping and Range of Ions in Matter*, (Pergamon, New York, 1985).

[18] P. Taras and B. Haas, Nucl. Instrum. Methods **123**, 73 (1975).

[19] Boris V. Pritychenko, Ph.D. dissertation, Michigan State University, 2000.

[20] Krishichayan, A. Chakraborty, S. Mukhopadhyay, S. Ray, N. S. Pattabiraman, S. S. Ghugre,

R. Goswami, A. K. Sinha, S. Sarkar, U. Garg, P. D. Madhusudhana, S. K. Basu, B. K. Yogi, L. Chaturvedi, A. Dhal, R. K. Sinha, M. Saha Sarkar, S. Saha, R. Singh, R. K. Bhomik, A. Jhingan, N. Madhavan, S. Muralithar, S. Nath, R. P. Singh, and P. Sugathan, Eur. Phys. J. A **29**, 151 (2006).

[21] P. J. R. Mason and P. H. Regan, private communication (2011).

[22] G. Audi, A. H. Wapstra, and G. Thibault, Nucl. Phys. **A729**, 337 (2003).

[23] P. M. Endt, Nucl. Phys. **A521**,1 (1990)

[24] P. M. Endt, Nucl. Phys. **A633**,1 (1998)

[25] L. K. Fifield, W. N. Catford, N. A. Orr, T. R. Ophel, A. Etchegoyen, and M. C. Etchegoyen, Nucl. Phys. **A552**, 125 (1993).

[26] J. P. Dufour, R. Del Moral, A. Fleury, F. Hubert, D. Jean, M. S. Pravikoff, H. Delagrange, H. Geissel, and K.-H. Schmidt, Z. Phys. **A324**, 487 (1986).

[27] S. M. Brown, W. N. Carford, J. S. Thomas, B. Fernández-Domínguez, N. A. Orr, M. Labiche, M. Rejmund, N. L. Achouri, H. Al Falou, N. I. Ashwood, D. Beaumel, Y. Blumenfeld, B. A. Brown, R. Chapman, M. Chartier, N. Curtis, G. de France, N. de Sereville, F. Delaunay, A. Drouart, C. Force, S. Franchoo, J. Guillot, P. Haigh, F. Hammache, V. Lapoux, R. C. Lemmon, A. Leprince, F. Maréchal, X. Mougeot, B. Mouginot, L. Nalpas, A. Navin, N. P. Patterson, B. Pietras, E. C. Pollacco, A. Ramus, J. A. Scarpaci, I. Stefan, and G. L. Wilson, Phys. Rev. C **85**, 011302(R) (2012).

[28] F. Nowacki and A. Poves, Phys. Rev. C **79**, 014310 (2009).

[29] T. A. Hinners, Vandana Tripathi, S. L. Tabor, A. Volya, P. C. Bender, C. R. Hoffman, Sangjin Lee, M. Perry, P. F. Mantica, A. D. Davies, S. N. Liddick, W. F. Mueller, A. Stolz, and B. E. Tomlin, Phys. Rev. C **77**, 034305 (2008).